

A HYSTERETIC SINGLE COOPER PAIR TRANSISTOR FOR SINGLE SHOT READING OF A CHARGE-QUBIT

Audrey Cottet, Denis Vion, Philippe Joyez, Daniel Esteve, and Michel H. Devoret*

1. INTRODUCTION

Superconducting nano-electronic devices are appealing candidates for implementing quantum-bits¹ (qubit) because they can be fabricated in parallel using lithography techniques. At the present time, the most advanced qubits are the single Cooper pair box² (CPB), which involves charge states of a small superconducting island, the RF-SQUID³ and the 3-junction SQUID⁴. Recently, Nakamura⁵ *et al.* demonstrated temporal coherence of quantum superpositions of qubit states in the CPB. The decay of Cooper pairs into quasiparticles used in this experiment for measuring the CPB is far from providing a single shot readout, and severely limits the coherence time of the superposition of states. Achieving single shot determination of the qubit energy eigenstate while preserving the coherence prior to measurement is a central issue. Recently, fast electrometers^{6,7,8,9} have been developed for measuring the charge of the CPB island, and the sensitivity necessary for such single-shot readout has already been reached by an electrometer based on the radio-frequency Single Electron Transistor. In this work, we present a new readout scheme based on the single Cooper Pair Transistor^{10,11,12} (CPT). In this superconducting device, the supercurrent is modulated by the charge coupled to the transistor island. We have measured the charge resolution of such an electrometer, and evaluated the back-action it would have on a CPB.

* All authors, Service de Physique de l'Etat Condensé, CEA-Saclay, F91191 Gif-sur-Yvette, France

2. PRINCIPLE OF THE READOUT

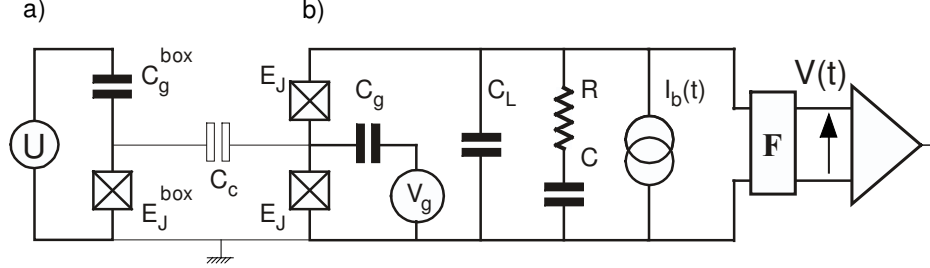


Figure 1. The single Cooper pair box (a) is a charge qubit. A natural readout scheme is to couple it to an electrometer through a capacitor C_c . The electrometer (b) tested in this work is a Cooper pair transistor (CPT). The transistor is current biased and damped only at AC frequencies.

2.1 The Cooper Pair Box as a Charge Qubit

The CPB² is schematically represented on Fig. 1a. It consists of a superconducting island coupled to a voltage source U through a Josephson junction with capacitance C_J^{box} and Josephson energy E_J^{box} , and through a small capacitance C_g^{box} . When the superconducting gap is larger than the charging energy $E_c^{box} = e^2 / 2C_\Sigma^{box}$, where C_Σ^{box} is the total capacitance of the island, the two lowest energy states of the CPB are superpositions of charge states $|n\rangle$, where n is an even number of electrons in the island. When the reduced gate charge $n_g^{box} = C_g^{box}U/e$ is close to an odd integer n_0 , and if E_J^{box} / E_c^{box} is small, the system behaves at low energy like an effective two level system. In the subspace spanned by $(|n = n_0 - 1\rangle, |n = n_0 + 1\rangle)$, the Hamiltonian is that of a spin $1/2$ in an effective field:

$$H_{box} = -\frac{1}{2}\vec{B}\cdot\vec{\sigma}, \quad (1)$$

where $\vec{\sigma} = [\sigma_x, \sigma_y, \sigma_z]$ is the Pauli matrices vector, and $B = [E_J^{box}, 0, 4E_c^{box}(1 - n_g^{box})]$. The ground and excited eigenstates of this Hamiltonian are the two states $|qb0\rangle$ and $|qb1\rangle$ of the qubit, indexed by 0 and 1 in this paper. The energy difference is $\hbar\Omega = E_J^{box} / \sin\theta$, and the charge difference obeys $\Delta n_{01} = \langle n \rangle_1 - \langle n \rangle_0 = 2\cos\theta$, where θ is the angle between \vec{B} and \vec{z} . Ideally, when the island charge of a generic state $\alpha|qb0\rangle + \beta|qb1\rangle$ is measured, the state is projected on $|qb0\rangle$ or $|qb1\rangle$ with the probabilities $|\alpha|^2$ and $|\beta|^2$.

2.2 The Single Cooper Pair Transistor as an Electrometer

A schematic representation of the CPT and of the bias circuitry we have implemented in our experiment is shown in Fig. 1b. The CPT^{10,12,12} itself consists of a superconducting island coupled to two superconducting reservoirs through two nominally identical small Josephson junctions with capacitance C_J and Josephson energy E_J , and coupled to a gate voltage source V_g through a small capacitance C_g . Its charging energy is $E_c = e^2 / 2C_\Sigma$, where C_Σ is the total capacitance of its island. Nominally, the CPT has two dimensionless control parameters: the gate charge $n_g = C_g V_g / e$ and the superconducting phase difference $\phi = \int v dt / \varphi_0$, where v is the voltage across the transistor and $\varphi_0 = \hbar / 2e$. The energy spectrum of the CPT is that of a CPB with effective Josephson energy $2E |\cos(\phi/2)|$. In the ground state with energy $E_0(n_g, \phi)$, the electrical potential of the island with respect to ground (see Fig. 1) is $V_I(n_g, \phi) = (1/e) \partial E_0 / \partial n_g$, and the supercurrent through the CPT is $I(n_g, \phi) = (1/\varphi_0) \partial E_0 / \partial \phi$. These quantities are both $2e$ periodic in n_g and 2π periodic in ϕ .

The CPT can be seen as an effective Josephson junction whose critical current $I_c(n_g) = \text{Max}_\phi [I(n_g, \phi)]$ is periodically modulated by the gate charge, and whose current-phase relation $I = I_c(n_g) f(n_g, \phi)$ is not strictly sinusoidal. This charge-induced variation of I is used for electrometry. It can be characterized by the dimensionless "gains" $g(n_g, \phi) = \partial \ln(I) / \partial n_g$ and $g_0(n_g) = \partial \ln(I_c) / \partial n_g$. These gains are maximal close to $n_g = 1[\text{mod } 2]$. The optimal sensitivity is obtained when $E_c \approx E_J$, with a gate modulation of I_c larger than 50% and $g_0 \approx 2$.

The CPT is a transducer obeying the reciprocity relation linking the phase dependence of the island potential and the gate charge dependence of the current:

$$\frac{\partial V_I}{\partial \phi} = \frac{R_k}{4\pi} \frac{\partial I}{\partial n_g}, \quad (2)$$

where $R_k = h/e^2$ is the resistance quantum.

In order to turn this transducer into an electrometer, it has to be embedded in a circuit which will perform a measurement of the supercurrent I . In a previous experiment, the CPT was voltage biased with a small shunt resistor, and the supercurrent measured with a SQUID array amplifier⁸. For this scheme, the sensitivity was limited by the SQUID amplifier to about $3 \cdot 10^{-4} \text{ e/Hz}^{1/2}$, within a 10 MHz bandwidth. In the present experiment, we use a current-biasing scheme like in conventional measurement setups, for which the zero-voltage branch of the characteristics is metastable. The working principle of our electrometer is to determine the gate dependent current required to induce the switching transition out of the zero-voltage state, during a given measuring time and with a given probability.

2.3 Switching of the CPT during a Current Pulse

Like in the case of a Josephson junction, the dynamics of the phase across a current-biased CPT is that of a particle in a tilted washboard potential, and subject to friction due to the impedance across the transistor. The mass of the particle and its velocity are proportional to the capacitance and the voltage, respectively. At $s(n_g) = I_b / I_c(n_g) < 1$, the potential has metastable minima from which the particle escapes by thermal activation. Note that here, an escape event does not always trigger the switching to the voltage state. The key point is that dissipation, which governs whether the particle will be retrapped in the next well or not, depends here strongly on the velocity. Switching occurs when the particle reaches a critical velocity which is determined by the difference between the actual tilt $s(n_g)$ and a critical tilt $s_{\max} < 1$: This process corresponds to an activation above a "dissipation barrier"¹³ as the greater the dissipation, the greater s_{\max} is. We introduce the switching rate $\Gamma[s(n_g), s_{\max}]$ which depends on the impedance and temperature.

The measurement of Γ at a given tilt is performed directly by applying a square bias-current pulse with amplitude $s(n_g)$ and duration t_{meas} . The probability that the system switches to the voltage-state is $p[s(n_g), s_{\max}, t_{\text{meas}}] = 1 - \exp[-\Gamma t_{\text{meas}}]$. We operate the device with I_b and n_g chosen such that $p[s(n_{g0}), s_{\max}, t_{\text{meas}}] = 0.5$. We exploit the steepness of p with respect to n_g : Depending whether n_g is above or below n_{g0} , the device will essentially switch or not. The CPT is thus here a threshold charge detector.

2.4 Theoretical Sensitivity

The charge resolution defined as $\Delta n_g(t_{\text{meas}}) = (dp / dn_g)_{n_{g0}}^{-1}$ is given by:

$$\Delta n_g(t_{\text{meas}}) = \frac{2}{\ln 2} \frac{1}{g_0(n_{g0})} \frac{1}{s(n_{g0}) \partial \ln(\Gamma) / \partial s}. \quad (3)$$

We estimate the associated error probability $er = p(n_{g0} - \Delta n_g / 2)$ to be 0.15. Note that the resolution Δn_g does not improve with the measurement time as $\sqrt{t_{\text{meas}}}$, like in the case of linear amplifiers. Nevertheless, for the sake of comparison, one can define an equivalent sensitivity as the input noise spectral density $S_{n_g} = 0.47 \Delta n_g^2 t_{\text{meas}}$ of a linear amplifier, which would result in the same error probability for the same measuring time.

Optimizing the CPT sensitivity requires maximizing $s(n_{g0}) \partial \ln(\Gamma) / \partial s$. In a previous work¹³, we have shown that both the reduced switching current s and the logarithmic derivative $\partial \ln(\Gamma) / \partial s$ of a small effective Josephson junction can be

maximized by damping the dynamics of the phase at ac frequencies with an RC circuit in parallel with the junction, as shown in Fig. 2. The charge resolution can be as small as desired by increasing the damping, but this gain is done at the expense of increased measuring time and back-action.

2.5 Numerical Simulations

In the case of a small Josephson junction, the switching rate Γ is analytically calculable in some limit cases, and approximate expressions are available^{13,14}. In the case of the CPT, one has to rely on numerical simulations of the system dynamics to determine the sensitivity. The dynamics of the phase across the CPT is governed by the system of Langevin equations¹³:

$$\begin{cases} \dot{\phi} = u_L = u + \alpha \dot{u} + \eta \\ s - f(n_g, \phi) = \alpha (\dot{u} + \varepsilon \dot{u}_L) \end{cases} \quad (4)$$

where u and u_L are the voltages across C and C_L in units of $R I_c$, $\alpha = R^2 C I_c / \varphi_0$ and $\varepsilon = C_L / C$; \dot{x} denotes the derivative of x with respect to the reduced time $\tau = R I_c t / \varphi_0$, and η is the reduced Johnson voltage noise across resistor R , which verifies $\langle \eta(0) \eta(\tau) \rangle = (2 k_B T / \varphi_0 I_c) \delta(\tau)$. We have numerically integrated Eqs. (4) for bias-current linear ramps and square pulses. In the case of a linear ramp, s is increased starting from a small value until u exceeds a threshold value u_{th} , the last s defining the reduced switching current I_s / I_c . In the case of a pulse, s is kept constant and the system is considered as having switched if u exceeds u_{th} before the end of the pulse. The result of these numerical experiments does not depend on the exact value chosen for u_{th} since the acceleration during the switching is very fast. The simulation determines the average switching current $\langle I_s \rangle$ for linear ramps, or directly the switching probability for bias-current pulses.

3. EXPERIMENT

3.1 Experimental Setup

We have fabricated a CPT on a thermally oxidized Si chip using 3-angle evaporation through a shadow mask¹⁵. The two first layers form the aluminum CPT, and the third layer forms the gold connecting leads. These non-superconducting leads provide dumps for out-of-equilibrium quasiparticles present in the superconducting electrodes. The leads, with estimated total parasitic capacitance to ground $C_L \approx 0.75$ pF, are wire-

bonded to a printed circuit board. Surface mounted components implementing the AC shunt ($R = 400\Omega$ and $C = 180pF$) of Fig. 2 are fitted onto this PCB. The CPT junctions have an area of $70 \times 90 \text{ nm}^2$, the asymmetry being smaller than 10%. The circuit was mounted in a shielded box fitted with SMA coaxial connectors. The bias, gate and measuring lines ending at these connectors were carefully filtered with copper powder and microfabricated RC filters¹⁶. The sample was current biased through a $100 \text{ k}\Omega$ resistor placed on the PCB, and its voltage was measured using a room temperature low noise amplifier. The gap voltage of the aluminum electrodes $\Delta = 170 \pm 5 \mu\text{eV}$, and the total CPT tunnel resistance $2R_T = 15.3 \pm 0.1 \text{ k}\Omega$ were deduced from large-scale I-V characteristics. The Josephson energy $E_J = 0.82 k_B K$ of each junction was calculated from the Ambegaokar-Baratoff's relation assuming no asymmetry between the junctions.

3.2 Input and Output Signals

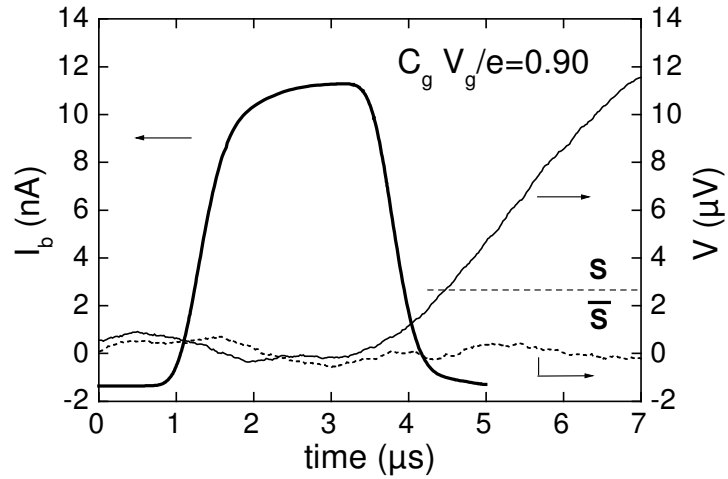


Figure 2. Bias-current pulse applied to the CPT, and voltage at the input of the amplifier for events where the transistor switches (solid line) or does not (dotted line). The dashed line indicates the threshold voltage used to discriminate the two types of events.

An arbitrary waveform voltage source was connected to the bias-current line. The frequency dependent transmission of the bias-current line was carefully calibrated, and the pulses were adjusted so as to provide a shape of the bias-current pulse as close as possible to a square wave. Figure 2 shows the bias-current pulses resulting from this adjustment. Switching always occurs when the bias-current is within to 10% of the maximum value I_P , and we can take $t_{meas} = 1 - 2 \mu\text{s}$. Figure 2 also shows the time evolution of the voltage V for events where the CPT switches or does not. The observed

voltage rise is well explained by the total capacitance of the measuring line including filters (represented by F in Fig. 1b), which is about 0.8 nF. The threshold voltage (see dashed line on Fig. 2) used to discriminate a switching event from a non-switching one was chosen sufficiently larger than the voltage noise to avoid false switching events while minimizing heating. The pulses were repeated with a frequency of 40 kHz, which corresponds to a duty cycle of 2/25.

3.3 Gate Modulation

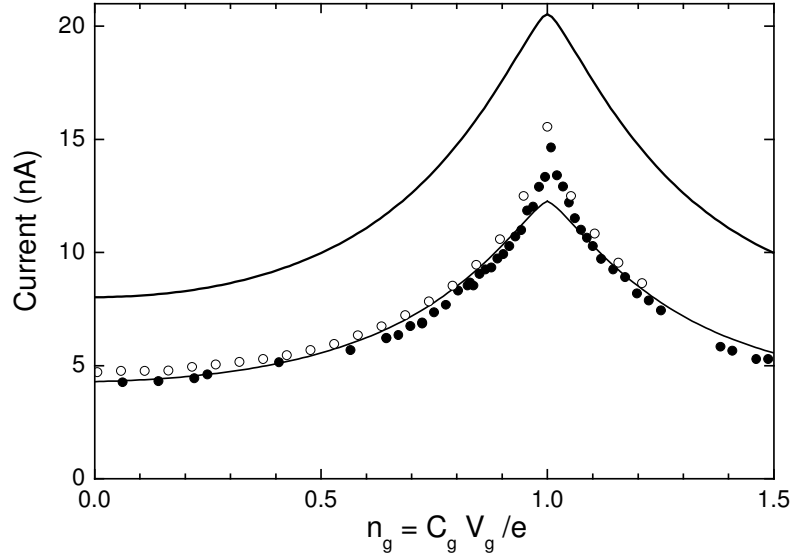


Figure 3. Gate modulation of the supercurrent of a CPT with $E_c = 1.12 k_B K$ and $E_J^* = 0.96 k_B K$. Solid symbols: average switching current measured at $T = 45$ mK by the ramp technique with $dI/dt = 87$ pA/ μ s and 14000 events per data point; bottom curve: average switching current predicted from numerical simulations for the same parameters. Open symbols: Current pulse height I_p resulting at 20 mK in a 50% switching probability for pulses with the same duration as that shown in Fig. 2, and 5000 events per point. Top curve: Theoretical critical current I_c .

The gate modulation of the switching current was first measured by the standard bias-current ramp technique¹⁷. An experimental modulation pattern $\langle I_s \rangle(n_g)$ is shown in Fig. 3, together with the predicted critical current $I_c(n_g)$, and the corresponding $\langle I \rangle(n_g)$ curve determined by simulation. The single fitting parameter is $E_c = 1.12 k_B K$, for which the experimental and simulated $\langle I_s \rangle$ coincide at $n_g = 0$ (a renormalization of the bare Josephson energy¹⁸ up to $E_J = 0.96 k_B K$ by charging effects has been taken into account). The E_c value agrees with the capacitance estimated from scanning electron micrographs. The experimental and simulated modulation curves

agree quantitatively except in a narrow region around $n_g = 1$, where the simulated $\langle I_s \rangle$ is 17 % lower than the experimental one. This discrepancy is not fully understood yet.

For measurements using the pulse technique, a digital feedback loop was used to vary the peak value I of the pulses to maintain the switching probability at 50%. The resulting gate modulation $I_p(n_g, p = 0.5)$ is also shown on Fig. 3.

3.4 Sensitivity

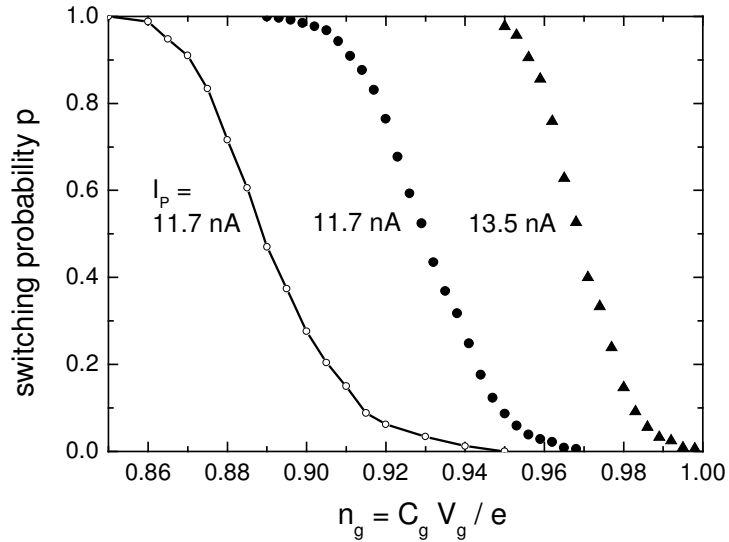


Figure 4. Experimental (solid symbols) and numerically simulated (open symbols) gate variation of the switching probability obtained with bias-current pulses as shown in Fig. 2. Peak currents are indicated for each data set. Each point is the result of an average over 500 (simulation) or 5000 (experiment) pulses. The steepest experimental gate variation (triangles) is obtained around $n_g = 0.97$ and leads to an experimental charge sensitivity of $2 \cdot 10^{-5} \text{ e/Hz}^{1/2}$.

Experimental and simulated $p(n_g)$ curves obtained for different I corresponding to n_{g0} values close to 1, for which the sensitivity is maximal, are shown in Fig. 4. The best experimental sensitivity was obtained at $n_g = 0.97$ with $I_p = 13.5 \text{ nA}$ (triangles on Fig. 4). In these conditions, according to the definitions of section 2.3, $\Delta n_g = 0.021$ and $S_{n_g}^{1/2} \approx 2 \cdot 10^{-5} \text{ e/Hz}^{1/2}$. Apart from a slight offset, the numerical simulation well reproduces the experimental curve $p(n_g)$ at $I_p = 11.7 \text{ nA}$. This shows that the sensitivity of the device is indeed limited by thermally activated switching and not by

noise. The achieved sensitivity is not the ultimate value, and can still be improved by increasing the damping. A gain in sensitivity by a factor 5 could be reached by implementing the RC shunt directly on chip, so that the parasitic capacitance C_L is almost suppressed (simulation not shown). However, for the purpose of qubit readout, sensitivity and back-action have to be optimized jointly. When back-action is taken into account, the capacitor C_L is found necessary, as shown in the following section.

In order to measure a CPB, the transistor island has to be connected to the box island by a coupling capacitor C_c (see Fig.1). The charge difference which has to be discriminated corresponds to $\kappa_1 \Delta n_{01}(\theta)$, where $\kappa_1 = C_c / C_\Sigma$ is the coupling factor between the CPT and the CPB. The condition for a single shot readout, i.e. readout with an error probability lower than our standard 15% (see above), is thus:

$$\kappa_1 > \kappa_{1 \min} = \Delta n_g(t_{meas}) / 2 \cos \theta . \quad (5)$$

For instance, a coupling κ_1 of 2% would be enough to measure a CPB with $\theta = \pi/4$ with one $2\mu\text{s}$ long pulse.

4. Back-action onto a Charge Qubit

A readout amplifier induces decoherence of the measured qubit. In the case where an explicit Hamiltonian of the system {qubit + readout} can be handled, this phenomenon can be described by computing the time evolution of the density matrix¹⁹. However, in the case of a CPB coupled to an electrometer, it is possible to follow a simpler approach. When the temperature is above 10 mK, it can be shown⁸ that decoherence is dominated only by dephasing induced by the thermal noise of its environment. Moreover, when the qubit environment is at low temperature, relaxation of the qubit from its excited state is much more probable than the opposite excitation⁸. The back-action of the readout is thus characterized by only 4 characteristic times T_φ^{OFF} , T_1^{OFF} , T_φ^{ON} , and T_1^{ON} describing dephasing and relaxation, in the OFF and ON states of the readout, respectively. These times have to fulfill several requirements for qubit manipulation and readout. Both T_φ^O and T_1^O should be long enough to allow coherent evolution prior to measurement, and T_1^{ON} should be longer than the measuring time t_{meas} , so that the information is not lost before the measurement is completed. The value of T_φ^{ON} is less important since quantum mechanics imposes anyway full decoherence in a projective measurement. The comparison of T_φ^{ON} with t_{meas} provides nevertheless an estimate of the readout ideality.

4.1 Dephasing due to Readout Back-action Noise

In the same way as the CPB island potential acts on the CPT supercurrent, the electrical potential $V_I(n, \phi)$ of the CPT island reacts on the CPB as a perturbing gate charge. Due to the Johnson noise in the resistor R , the phase ϕ across the CPT fluctuates according to Eqs. (4), and the CPT converts this phase fluctuation into a fluctuation δV_I of its island potential. The box gate charge fluctuates by $\delta n_g^{box} = \kappa_2 \delta v_I$, where $\kappa_2 = C_c / C_\Sigma^{box}$ and $\delta v_I = C_\Sigma \delta V_I / e$, inducing fluctuations of the CPB transition frequency. A coherent superposition of qubit states would thus accumulate a random phase at a rate $d\Delta\varphi / dt = A \delta v_I$, with $A = 4\kappa_2 E_c^{box} \cos \theta / \hbar$. If the fluctuating voltage δv_I is gaussian, the coherence factor $\langle e^{i\Delta\varphi(t)} \rangle$ at time t is given by:

$$\langle e^{i\Delta\varphi(t)} \rangle = e^{-\frac{\langle \Delta\varphi(t)^2 \rangle}{2}},$$

$$\text{with } \langle \Delta\varphi(t)^2 \rangle = A^2 t^2 \int_0^\infty S_{v_I}(\omega) \text{sinc}^2(\omega t / 2) d\omega. \quad (6)$$

Here, $S_{v_I}(\omega)$ is the spectral density* of the CPT island voltage fluctuations. The time dependence of the coherence factor is exponential at long times only when the spectral density is constant below some characteristic frequency ω_c . At times longer than ω_c^{-1} , the dephasing time T_φ^{ON} is given by:

$$T_\varphi^{ON} = \frac{2}{\pi A^2 S_{v_I}(\omega = 0)}. \quad (7)$$

When the readout is OFF ($I_b \ll I_p$), the phase ϕ fluctuates in the vicinity of one of the minima of the washboard potential, located at $\phi_0 = \arcsin I_b / I_c \text{ [mod } 2\pi]$, and Eqs. (4) can be linearized around ϕ_0 . Using Eq. (2), one obtains for the spectral density:

$$S_{v_I}^{OFF}(\omega) \approx \frac{2}{\pi} \left(\frac{\hbar}{4E_c} \frac{g}{l} \right)^2 \frac{k_B T}{R e^2} \frac{1}{1 + \frac{1}{(RC\omega)^2}}, \quad (8)$$

where $l = \partial \ln(f) / \partial \phi$. Using Eq. (6), one gets:

$$\frac{\langle \Delta\varphi(t)^2 \rangle^{OFF}}{2} = \frac{t}{\tau_\varphi^{OFF}} \frac{1 - e^{-t/RC}}{t/RC}, \quad (9)$$

* We use here only "engineer" spectral densities corresponding to the power density at a positive pulsation.

where

$$\tau_{\varphi}^{OFF^{-1}} = \left(\kappa_2 \cos \theta \frac{E_c^{box}}{E_c} \frac{g}{l} \right)^2 \frac{k_B T}{R e^2} . \quad (10)$$

Since the spectral density is zero at zero frequency, decoherence stays finite. The coherence factor thus saturates at a value $\langle e^{i\Delta\varphi(t)} \rangle = e^{-R U / \tau_{\varphi}^{OFF}}$ for times longer than RC . For the parameters we consider, $RC \ll \tau_{\varphi}^{OFF}$. Dephasing due to the CPT in the OFF state is thus negligible.

When the readout is ON, the excursions of the phase ϕ are no longer bounded. The spectral density $S_{v_I}(\omega)$ can be obtained from simulations, using the constitutive relation $V_I(n_g, \phi)$. It is constant at low frequency, which leads to an exponential decay for the coherence factor with a time constant T_{φ}^{ON} .

Table 1 treats the case of a CPB with $E_J^{box} = E_c^{box} = 0.5k_B K$, coupled to the readout with $\kappa_2 \approx \kappa_{1 \min} / 2 = 1\%$ and displays T_{φ}^{ON} and t_{meas} calculated from Eqs. (9)-(10). Since $t_{meas} / T_{\varphi}^{ON} \sim 20$, the readout is far from reaching the ideal quantum measurement limit. Although we have only considered here the contribution of the CPT to dephasing, one should not forget that the dominant dephasing source in the CPB is the offset charge noise, which is due to the random motion of charges at the microscopic level.

Table 1. Estimated coherence time T_{φ} and relaxation time T_1 of a CPB ($E_J = E_c = 0.5k_B K$) if it were coupled to the readout of our experiment with $\kappa_2 \approx 1\%$. Decoherence sources other than the readout have not been considered. Operating conditions are indicated on the first line. The measurement time t_{meas} is given for comparison.

	OFF State		ON State
	$s = 0$ $\theta = \pi/2$	$s = 0.5$ $\theta = \pi/4$	$s = I_P / I_C \approx 0.7$ $\theta = \pi/4$
T_{φ}	∞	non-exponential decay $\tau_{\varphi} \sim 500 \mu\text{s}$ (see text)	$\sim 100 \text{ ns}$
T_1	∞	$\sim 200 \text{ ms}$	$\sim 60 \mu\text{s}$
t_{meas}	-	-	$< 2 \mu\text{s}$

4.2 Relaxation

We now discuss the relaxation of the CPB from $|qb1\rangle$ towards $|qb0\rangle$ at low temperature, accompanied by an energy transfer $\hbar\Omega$ into an electromagnetic mode Ω of the circuit. We assume here that the bandgap of the CPT is sufficiently higher than $\Omega/2\pi$, so that it stays in its ground state, and can be treated adiabatically. Within this framework, the CPT and its bias circuitry are equivalent to an effective impedance $Z_{eff}(\omega)$ connected to the CPB island. This impedance is given by:

$$Z_{eff}(\omega) = \frac{1}{jC_c\omega} \left(1 - \frac{\kappa_1}{2E_C} \left(\frac{\partial^2 E_0}{\partial n_g^2} - \frac{\varphi_0 g^2 I}{l} \frac{1}{1 + \frac{j\omega\varphi_0 Y(\omega)}{lI}} \right) \right)^{-1}, \quad (11)$$

where $Y(\omega)$ is the admittance in parallel with the CPT. The relaxation rate is then obtained from $Z_{eff}(\omega)$ using Fermi's golden rule:

$$\Gamma_1 = 4\pi\Omega \sin^2 \theta \kappa_2^2 \frac{\text{Re}[Z_{eff}(\Omega)]}{R_k}. \quad (12)$$

At $\phi = 0$, $g = 0$, $\text{Re}[Z_{eff}(\Omega)] = 0$, and no relaxation occurs at the lowest order. At $\phi \neq 0$, and for the external admittance $Y(\omega) = iC_L\omega + (iC\omega + R^{-1})^{-1}$ we consider, one has:

$$\frac{\text{Re}[Z_{eff}(\Omega)]}{R_K} = \frac{R_K}{R} \left(\frac{g}{4\pi l} \right)^2 \frac{1}{\left[\left(\frac{\Omega}{\omega_{c1}} \right)^2 - 1 \right]^2 + \left[\frac{\Omega}{\omega_{c1}} \right]^2}, \quad (13)$$

where $\omega_{c1} = \sqrt{\frac{\partial I / \partial \phi}{\varphi_0 C_L}}$ and $\omega_{c2} = R \frac{\partial I / \partial \phi}{\varphi_0}$ are cutoff angular frequencies of the system.

These expressions give an instantaneous rate depending on ϕ and n_g . They can be used directly to obtain the relaxation time $T_1(\phi) = 1/\Gamma_1$ when the readout is OFF, when the phase excursions are small. When the readout is ON, the system experiences a variable relaxation rate as the phase ϕ turns but an average can be performed, assuming equiprobability of ϕ . The resulting T_1^{ON} is displayed in Table 1 and verifies $T_1^{ON} / t_{meas} \sim 30$, what is compatible with a non-destructive measurement of the CPB. We have found that this relaxation time depends strongly on the external admittance. In

particular, the capacitor $C_L = 0.75 \text{ pF}$ provides a high frequency shunt that diminishes relaxation by a factor of about 10^3 . An improved design of the microwave impedance would probably allow a better sensitivity while keeping the relaxation time T_1^{ON} longer than t_{meas} .

5. CONCLUSION

We have fabricated and operated a new threshold charge detector based on the Cooper pair transistor. The best equivalent sensitivity we have obtained is $2 \cdot 10^{-5} \text{ e/Hz}^{1/2}$ in a 1MHz bandwidth. This detector, which is of the latching type and only requires simple room temperature electronics, could provide an efficient readout for a charge qubit. We have shown that, by proper engineering of the impedance in parallel with the Cooper pair transistor, this system meets the criteria for qubit operation and readout: dephasing and relaxation are negligible prior to readout, and relaxation during readout is small enough to allow discrimination of qubit states with signal to noise ratio of order 1.

6. REFERENCES

1. M. Nielsen and I. Chuang, *Quantum Computation and Quantum Information* (Cambridge University Press, Cambridge, 2000).
2. V. Bouchiat et al, *Physica-Scripta*, **76**, 165 (1998).
3. Siyuan-Han, R. Rouse, and J.E. Lukens, *Phys. Rev. Lett.*, **84**, 1300 (2000).
4. C.H. van der Wal et al., *Science*, **290**, 773 (2000).
5. Y. Nakamura, Y.A. Pashkin, and J.S. Tsai, *Nature*, **398**, 786 (1999) ; *Physica-B* **280**, 405(2000).
6. R.J. Schoelkopf et al., *Science*, **280**, 1238 (1998).
7. A. Aassime et al, *Phys. Rev. Lett.*, **86**, 15 (2001).
8. A. Cottet et al, in : *Macroscopic Quantum Coherence and Quantum Computing*, edited by D. Averin, B.Ruggiero, and P. Silvestrini (Kluwer Academic/Plenum Publisher , New York 2001), pp 111-125.
9. A.B. Zorin in this book.
10. T.A. Fulton and G.J. Dolan, *Phys. Rev. Lett.*, **59**, 109 (1987).
11. P. Joyez et al, *Phys. Rev. Lett.*, **72**, 2548 (1994).
12. A. B. Zorin, *Phys. Rev. Lett.*, **76**, 4408 (1996).
13. D. Vion et al, *Phys. Rev. Lett.*, **77**, 3435 (1996) ; P. Joyez et al, *J. of Superconductivity*. **12**, 757 (1999).
14. The theoretical sensitivity corresponding to very short current square pulses above S_{\max} will be published elsewhere.
15. G.J. Dolan and J.H. Dunsmuir, *Physica B*, **152**, 7 (1988).
16. D. Vion et al, *J. Appl. Phys.*, **77**, 2519 (1995).
17. T.A. Fulton and L.N. Dunkleberger, *Phys. Rev. B*, **9**, 4760 (1974).
18. P. Joyez, *Thesis*, Paris VI University, (1995).
19. A. Schnirman and G. Schön, *Phys Rev.*, *B* **57**, 15400 (1998).